Journal of Photochemistry and Photobiology A: Chemistry 210 (2010) 23–30

Contents lists available at ScienceDirect

Journal of Photochemistry and Photobiology A: Chemistry

journal homepage: www.elsevier.com/locate/jphotochem

On the quenching of MLCT luminescence by amines: The effect of nanoaggregation in the decrease of the reorganization energy

Larisa L.B. Bracco, Mario R. Féliz, Ezequiel Wolcan*

Instituto de Investigaciones Fisicoquímicas Teóricas y Aplicadas (INIFTA, UNLP, CCT La Plata-CONICET), Diag. 113 y 64, Sucursal 4, C.C. 16, B1900ZAA La Plata, Argentina

ARTICLE INFO

Article history:
Received 4 September 2009
Received in revised form
10 November 2009
Accepted 12 December 2009
Available online 4 January 2010

Keywords:
Amines
Rhenium
MLCT
Quenching
Spin–orbit coupling

ABSTRACT

The MLCT luminescence quenching of $pyRe(CO)_3bpy^+$ and/or the polymer $\{[(vpy)_2\text{-}vpyRe(CO)_3bpy]CF_3SO_3\}_{n-200}$ by amines proceeds via an electron transfer reaction which produces amine radical cations and $pyRe^I(CO)_3(bpy)^\bullet$/$-Re^I(CO)_3(bpy)^\bullet$, respectively. The quenching follows a typical Stern–Volmer kinetics for both $pyRe(CO)_3bpy^+$ and $\{[(vpy)_2\text{-}vpyRe(CO)_3bpy]CF_3SO_3\}_{n-200}$. The observed rate constants for the quenching of the Re^I-polymer luminescence by amines show "vestiges" of the inverted effect predicted by Marcus while the quenching of $pyRe(CO)_3bpy^+$ luminescence follow the Rehm–Weller type of behavior. The lower value obtained for the total reorganization energy of the Re^I-polymer than that for $pyRe(CO)_3bpy^+$ is rationalized in terms of the retarded solvent motions inside the nanoaggregates formed by the Re^I-polymer in acetonitrile solutions.

© 2009 Elsevier B.V. All rights reserved.

1. Introduction

Electron transfer reactions are distinguished by their ubiquity and by their essential roles in many physical, chemical and biological processes. Therefore, understanding the factors which determine electron transfer rates is of considerable importance. Kinetics of the electron transfer (ET) reactions is governed by different factors, like solvent environment, free energy of the reaction (ΔG) and electronic coupling factors. The most remarkable prediction of the Marcus theory [1] is that the ET rates should follow a parabolic dependence on ΔG. In the classical limit, for reactions in condensed media, theory predicts a bell-shaped Gibbs energy-rate relationship: rate constants are expected to be small for weakly exothermic reactions, increase to a maximum for moderately exothermic reactions (the *normal region*) and decrease for highly exothermic electron transfer reactions in the so-called *inverted region*. The theoretical prediction of this *inverted region* had generated a lot of controversy after its postulation, due to the lack of the experimental evidences and confirmation of the *inverted effect* took about 25 years [2]. After that the *inverted region* has been observed experimentally in many electron transfer systems [3–8]. Experimental evidence for the Marcus *inverted region* in the bimolecular ET reactions is however, very rare [9]. In most of these reactions, the variation in the ET rates with the ΔG of the reactions is seen to follow the Rehm–Weller type of behavior [10], mainly due to the influence of the diffusional rate of the reactants on the effective reaction rate. There are two main obstructions in observing the Marcus *inverted region* in bimolecular ET reactions, namely, (i) diffusion of the reactants and (ii) lack of availability of suitable donor–acceptor series to achieve very high reaction exothermicities. The first drawback may be reduced if ET is carried out in systems where reactants are confined into micelles and/or nanoaggregates and thus their movements will be highly restricted.

We have previously investigated solvent and temperature effects on the photophysical properties of the polymer $\{[(vpy)_2\text{-}vpyRe(CO)_3bpy]CF_3SO_3\}_{n-200}$ and the related $CF_3SO_3[pyRe(CO)_3bpy]$ complex (see Scheme 1). Differences between the polymer and $CF_3SO_3[pyRe(CO)_3bpy]$ photophysical behavior were rationalized in terms of solvent and thermal effects on the transition between rigid rod and coil structures of the Re^I-polymer [11a]. The formation of micelles has been reported in polystyrene *block*-poly(4-vinylpyridine) (PS-*b*-PVP) functionalized with pendants $-Re(CO)_3(bpy)^+$ groups. Two PS-*b*-PVP–$Re(CO)_3(bpy)^+$ polymers with different Re^I content exhibited the formation of rodlike and/or spherical micelles, as shown by transmission electron microscopy and light scattering experiments [12,13]. We have also reported the aggregation of single polymer molecules to form spherical nanodomains in acetonitrile solutions of the polymer $\{[(vpy)_2\text{-}vpyRe(CO)_3bpy]CF_3SO_3\}_{n-200}$ [14], hereafter denoted for simplicity

* Corresponding author at: Instituto de Investigaciones Fisicoquímicas Teóricas y Aplicadas (INIFTA, UNLP, CCT La Plata-CONICET), Diag. 113 y 64, Sucursal 4, C.C. 16, B1900ZAA La Plata, Argentina. Tel.: +54 221 4257430.
E-mail address: ewolcan@inifta.unlp.edu.ar (E. Wolcan).

1010-6030/$ – see front matter © 2009 Elsevier B.V. All rights reserved.
doi:10.1016/j.jphotochem.2009.12.010

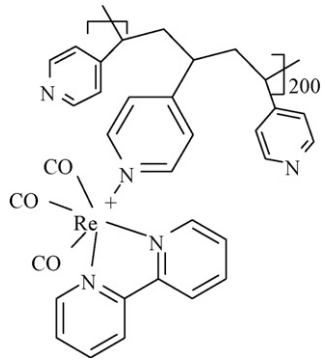

Scheme 1. Chemical structure of ReP4VPy.

as ReP4VPy. In this paper we study the photoinduced ET reaction between the metal-to-ligand charge transfer (MLCT) excited state of ReP4VPy and CF_3SO_3[pyRe(CO)$_3$bpy] by several amines used as sacrificial donors. The MLCT luminescence quenching of pyRe(CO)$_3$bpy$^+$ and/or ReP4VPy by amines proceeds via an electron transfer reaction which produces amine radical cations and pyRe^{I}(CO)$_3$(bpy)$^{\bullet}$/–Re^{I}(CO)$_3$(bpy)$^{\bullet}$, respectively. The observed rate constants for the quenching of the ReP4VPy luminescence by amines show "vestiges" of the inverted effect while the quenching of pyRe(CO)$_3$bpy$^+$ luminescence follows the Rehm–Weller type of behavior.

2. Materials and methods

2.1. Flash-photochemical procedures

Optical density changes occurring on a time scale longer than 10 ns were investigated with a flash photolysis apparatus described elsewhere [15–17]. In these experiments, 25 ns flashes of 351 nm (ca. 25–30 mJ/pulse) light were generated with a Lambda Physik SLL-200 excimer laser. The energy of the laser flash was attenuated to values equal to or lower than 20 mJ/pulse by absorbing some of the laser light by $Ni(ClO_4)_2$ solutions with appropriate optical transmittances, $T = I_t/I_0$, where I_0 and I_t are the intensities of the light arriving at and transmitted from the photolysis cell, respectively. The transmittance, $T = 10^{-A}$, was routinely calculated by using the spectrophotometrically measured absorbance, A, of the solution. A right angle configuration was used for the pump and the probe beams. Concentrations of the complexes were adjusted to provide homogeneous profiles of photogenerated intermediates over the probe beam optical path, $l = 1$ cm. To satisfy this optical condition, solutions were prepared with an absorbance equal to or less than 0.4 over the 0.2 cm optical path of the pump. All solutions used in the photochemical work were deaerated with streams of ultrahigh-purity N_2 before and during the irradiations.

2.2. Time-resolved luminescence quenching

The instrumentation for the time-resolved luminescence measurements has been described elsewhere [18]. Lifetime measurements were made at room temperature using a pulsed nitrogen laser with excitation at 337 nm and monitoring the signal at wavelengths between 500 and 560 nm. A modified 1P28 photomultiplier tube circuit with ca. 1 ns response time was used as the detector for the green emission dispersed through a monochromator. The signal was directly measured on a fast digitizing oscilloscope (Hewlett Packard Instruments) and the temporal resolution of the overall system was ca. 20 ns. Quenching of [pyRe(CO)$_3$bpy]CF_3SO_3 and the polymer $\{[(vpy)_2\text{-}vpyRe(CO)_3bpy]\ CF_3SO_3\}_{200}$ luminescence by different amines was investigated by varying the amine concentration between 1×10^{-5} and 2×10^{-2} M in acetonitrile at room temperature. Lifetime measurements were carried out on fresh solutions of the rhenium compounds ([Re] = 5×10^{-5} M) which had been deaerated by bubbling O_2-free N_2 containing increasing concentrations of the appropriate amine.

2.3. Pulse radiolysis

Pulse radiolysis experiments were carried out with a model TB-8/16-1S electron linear accelerator. The instrument and computerized data collection for time-resolved UV–vis spectroscopy and reaction kinetics have been described elsewhere in the literature [19,20]. Thiocyanate dosimetry was carried out at the beginning of each experimental session. Details of the dosimetry have been reported elsewhere [19,21]. The procedure is based on the concentration of $(SCN)_2^{\bullet-}$ radicals generated by the electron pulse in an N_2O-saturated 10^{-2} M SCN^- solution. In the procedure, the calculations were made with $G = 6.13$ and an extinction coefficient $\varepsilon = 7.58 \times 10^3\ M^{-1}\ cm^{-1}$ at 472 nm [19,21] for the $(SCN)_2^{\bullet-}$ radicals. In general, the experiments were carried out with doses that in N_2-saturated aqueous solutions resulted in $(2.0 \pm 0.1) \times 10^{-6}$ to $(6.0 \pm 0.3) \times 10^{-6}$ M concentrations of e^-_{aq}. In these experiments, solutions were deaerated with streams of the O_2-free N_2 or N_2O gasses. In order to irradiate a fresh sample with each pulse, an appropriate flow of the solution through the reaction cell was maintained during the experiment.

The radiolysis of CH_3OH and CH_3OH/H_2O mixtures with ionizing radiation has been reported elsewhere in the literature [22–24]. These studies have shown that pulse radiolysis can be used as a convenient source of e^-_{sol} and $C^{\bullet}H_2OH$ radicals according to Eq. (1)

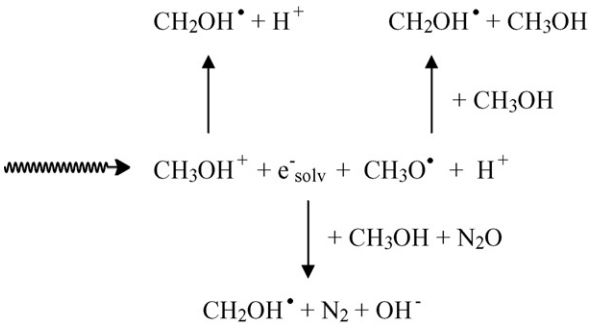

(1)

Since e^-_{sol} and $CH_2OH^{\bullet}$ have large reduction potentials, i.e., −2.8 V versus NHE for e^-_{sol} and −0.92 V versus NHE for $CH_2OH^{\bullet}$, they have been used for the reduction of coordination complexes and for the study of electron transfer reactions. The yield of e^-_{sol} in CH_3OH ($G \approx 1.1$) is about a third of the G value in the radiolysis of H_2O ($G \approx 2.8$) [22]. In solutions where e^-_{sol} was scavenged with N_2O [24], the $CH_2OH^{\bullet}$ radical appears to be the predominant product (yield >90%) of the reaction between CH_3OH and $O^{\bullet-}$.

2.4. General methods

UV–vis spectra were recorded on a Cary 3 spectrophotometer. Curve Fit analysis was performed using the non-linear curve fit tool of Origin 7.

2.5. Materials

The amine quenchers aniline, N,N,N′,N′-tetramethyl-1,4-phenylenediamine,1,4-phenylenediamine, 1,2-phenylenediamine, DABCO, N,N,N′,N′-tetramethylethylenediamine, N,N di-isopropylethylamine, di-isopropylamine, triethylamine, N,N,N′,N′-tetra-

Table 1
Quenching rate constants ($k_q \pm 2SE$) of MLCT excited states of ReP4VPy and pyRe(CO)$_3$(bpy)$^+$ in acetonitrile by aliphatic and aromatic amines.

Quencher	$E_{1/2}$ (V) (vs. SCE)	ΔG (eV)	ReP4VPy k_q (M^{-1} s^{-1})	pyRe(CO)$_3$(bpy)$^+$ k_q (M^{-1} s^{-1})
N,N,N′,N′-Tetramethyl 1,4-phenylenediamine	0.12[a]	−1.16	$(4.8 \pm 0.8) \times 10^9$	$(2.0 \pm 0.2) \times 10^{10}$
1,4-Phenylenediamine	0.26[a]	−1.02	$(1.1 \pm 0.6) \times 10^{10}$	$(1.3 \pm 0.1) \times 10^{10}$
1,2-Phenylenediamine	0.40[b]	−0.88	$(1.5 \pm 0.1) \times 10^{10}$	$(1.30 \pm 0.04) \times 10^{10}$
DABCO	0.56[d]	−0.72	$(7.8 \pm 0.8) \times 10^9$	$(1.02 \pm 0.02) \times 10^{10}$
N,N,N′,N′-Tetramethylethylenediamine	0.87[d]	−0.41	$(2.1 \pm 0.6) \times 10^9$	$(1.0 \pm 0.2) \times 10^9$
N,N-Di-isopropyl-ethylamine	0.89[d]	−0.39	$(6 \pm 1) \times 10^9$	$(5 \pm 1) \times 10^9$
Aniline	0.93[a]	−0.35	$(6.7 \pm 0.4) \times 10^9$	$(5.5 \pm 0.4) \times 10^9$
Triethylamine	0.99[d]	−0.29	$(2.1 \pm 0.2) \times 10^9$	$(1.00 \pm 0.06) \times 10^9$
N,N,N′,N′-Tetramethyldiaminomethane	1.06[d]	−0.22	$(5 \pm 1) \times 10^8$	$(2.45 \pm 0.06) \times 10^8$
Diethylamine	1.14[c]	−0.14	$(1.3 \pm 0.2) \times 10^8$	$(1.4 \pm 0.2) \times 10^8$
Di-isopropylamine	1.31[a]	0.03	$(1.1 \pm 0.2) \times 10^8$	$(2.6 \pm 0.2) \times 10^7$
Dibencylamine	1.36[c]	0.08	$(8 \pm 1) \times 10^6$	$(8 \pm 1) \times 10^6$
n-Butylamine	1.39[a]	0.11	$(1.3 \pm 0.1) \times 10^7$	$(6 \pm 1) \times 10^6$

[a] Ref. [30a].
[b] Ref. [30b].
[c] Ref. [30c].
[d] Ref. [31a].

methyldiaminomethane, diethylamine, dibencylamine, and n-butylamine purchased from Aldrich were of the highest purity available. When required they were purified by distillation. The pure amines were handled under nitrogen. The complex [pyRe(CO)$_3$bpy]CF_3SO_3 and ReP4VPy, were available from previous work [11].

3. Results and discussion

3.1. Forward electron transfer

The reductive quenching of the rhenium complex metal-to-ligand charge transfer (MLCT) excited state of [pyRe(CO)$_3$-bpy]CF_3SO_3 and polymer ReP4VPy by amines produces the oxidized form of the amine and the reduced radical of the rhenium complex (see below) (Eqs. (2) and (3))

$$[pyRe(CO)_3bpy^+]^* + NR_3 \xrightarrow{k_{q,1}} pyRe(CO)_3bpy^\bullet + NR_3^{\bullet+} \quad (2)$$

$$-[pyRe(CO)_3bpy^+]^* + NR_3 \xrightarrow{k_{q,2}} -Re(CO)_3bpy^\bullet + NR_3^{\bullet+} \quad (3)$$

where [pyRe(CO)$_3$bpy$^+$]* and –[Re(CO)$_3$bpy$^+$]* denote the MLCT excited states in pyRe(CO)$_3$bpy$^+$ and in a pendant –Re(CO)$_3$bpy$^+$ chromophore of polymer ReP4VPy and $k_{q,1}$ and $k_{q,2}$ denote the bimolecular rate constants for pyRe(CO)$_3$bpy$^+$ and ReP4VPy, respectively.

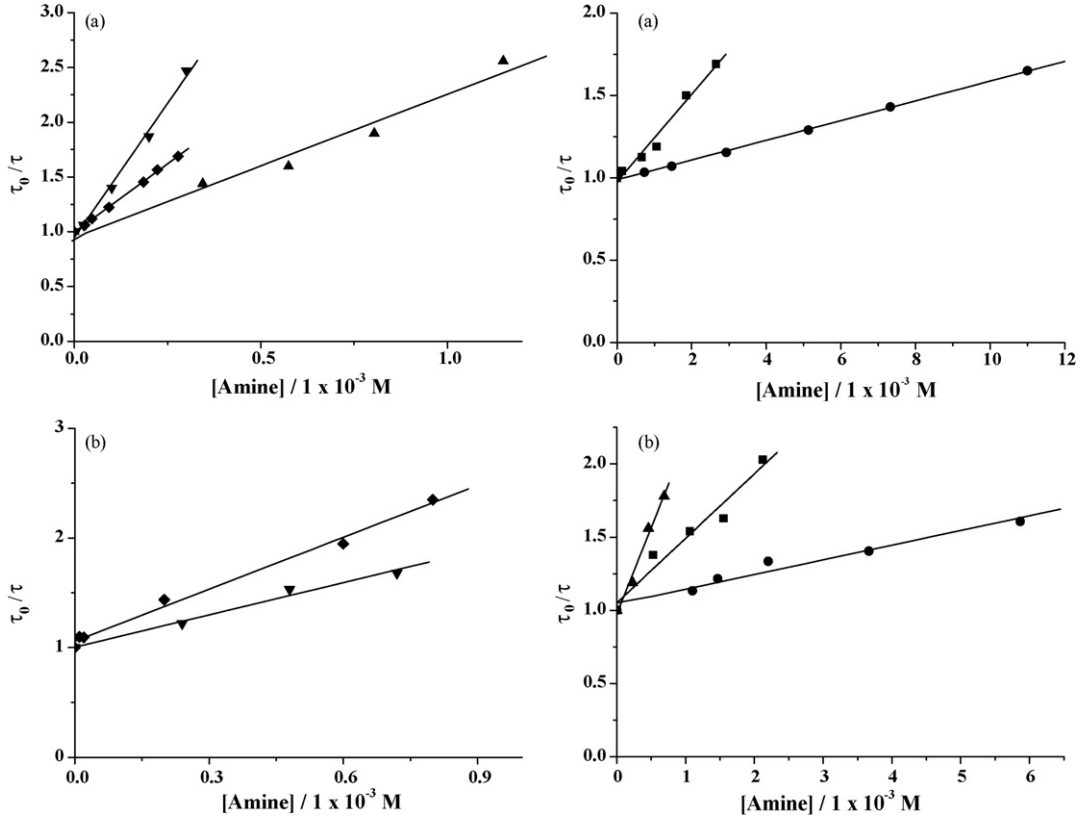

Fig. 1. Stern–Volmer kinetics for the MLCT luminescence quenching of (a) pyRe(CO)$_3$(bpy)$^+$ and (b) ReP4VPy by several amines: (■) N,N,N′,N′-tetramethylethylenediamine, (●) N,N,N′,N′-tetramethyldiaminomethane, (▲) N,N di-isopropyl-ethylamine, (▼) N,N,N′,N′-tetramethyl-1,4-phenylenediamine and (♦)DABCO.

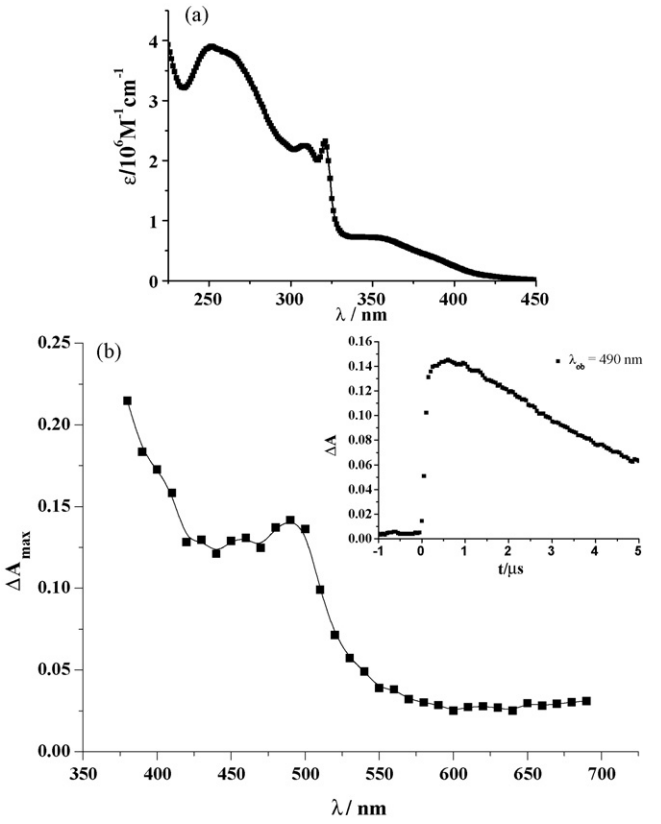

Fig. 2. (a) Steady state absorption spectrum of ReP4VPy. (b) Transient spectra recorded at a delay of 0.6 μs after the laser pulse (showing maximum absorbance change, ΔA_{max}) in flash photolysis experiments of ReP4VPy ($[Re^I] = 5 \times 10^{-4}$ M) in deaerated CH_3CN containing TEA 0.1 M. Inset shows an oscilographic trace at λ_{ob} = 490 nm. See text for details.

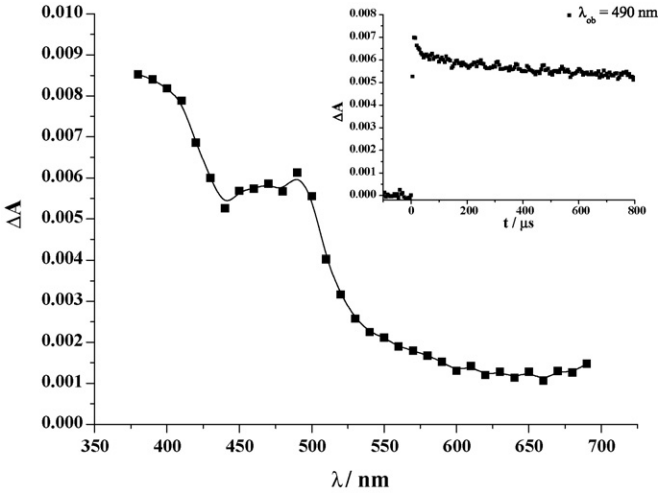

Fig. 3. Transient spectra recorded at a delay of 50 μs after the radiolytic pulse in pulse radiolysis experiments of N_2-deaerated methanolic solutions of ReP4VPy. Inset shows an oscilographic trace at λ_{ob} = 490 nm. See text for details.

The results of the quenching experiments are shown in Table 1. The data were plotted according to the Stern–Volmer equation (Eq. (4))

$$\frac{\tau_0}{\tau} = 1 + k_q \tau_0 [NR_3] \quad (4)$$

where τ_0 is the excited state lifetime in the absence of quencher and τ is the luminescence lifetime at the presence of quencher. The plots were linear over the range of quencher concentrations used and the intercepts were unity as expected (Fig. 1). The k_q values, collected in Table 1, were determined from the slopes of the lines using τ_0 = 245 and 203 ns for [pyRe(CO)$_3$bpy]CF_3SO_3 and ReP4VPy, respectively [11a].

3.2. Species formed by the photochemical and thermal reduction of ReP4VPy

Transient absorption spectra in the 15 ns to microsecond time domain were recorded with a 351 nm excimer laser flash photolysis set-up. The irradiation of the polymer at 351 nm produces transient spectra with the absorption bands of the –Re^I(CO)$_3$(bpy)$^+$ MLCT excited state [11a]. When a sacrificial reductant is present in the solution, the MLCT excited state is quenched by an electron transfer reaction. Therefore, the reductive quenching of the MLCT excited state was investigated using the flash photolysis technique with deaerated ReP4VPy ($[Re^I] = 5 \times 10^{-4}$ M) solutions in CH_3CN containing triethylamine (TEA) as the excited state quencher. Transient spectra displaying two absorption bands with λ_{max} = 450 and 490 nm were recorded with [TEA] = 0.1 M (Fig. 2). The spectral features of Fig. 2 are very similar to the spectrum attributed to [ReBr(CO)$_3$(bpy)]$^{\bullet -}$ [25]. There is ample precedent [25] to suggest that the added electron in this reduced complex resides in an orbital localized to a significant extent on the bpy ligand. Consequently, the reduced species can be viewed in a formal sense as a Re^I center bound to a 2,2′-bipyridine radical anion, i.e., [ReBr(CO)$_3$(bpy$^{\bullet -}$)]. As a result, the spectral features of Fig. 2 might correspond to absorptions of the bpy$^{\bullet -}$ ligand in the chromophore –Re^I(CO)$_3$(bpy)$^{\bullet}$. Therefore, the spectra in Fig. 2 could be attributed to the photogeneration of pendant –Re^I(CO)$_3$(bpy)$^{\bullet}$ chromophores. A growth of the –Re^I(CO)$_3$(bpy)$^{\bullet}$ spectrum that showed an additional reduction of –Re^I(CO)$_3$(bpy)$^+$ groups by reducing radicals derived from TEA oxidation in the polymer may be observed also in Fig. 2 (inset). The prompt growth of the –Re^I(CO)$_3$(bpy)$^{\bullet}$ spectrum was followed by a rapid decay of the spectrum with a first-order kinetics with a lifetime of $\tau = 4.8 \pm 0.2$ μs.

To confirm the assignment of the transient recorded in Fig. 2 to the photogeneration of pendant –Re^I(CO)$_3$(bpy)$^{\bullet}$ chromophores, the same chromophores were generated by pulse radiolysis of ReP4VPy ($[Re^I] = 2 \times 10^{-4}$ M) in MeOH deaerated with streams of N_2. The reaction between e^-_{solv} and ReP4VPy was completed within the first microsecond after the radiolytic pulse with a rate constant $k = (1.1 \pm 0.1) \times 10^{10}$ M^{-1} s^{-1}. The transient spectrum that is generated by the e^-_{solv} reaction (Fig. 3) exhibited two absorption bands with λ_{max} = 450 and 490 nm. It bears a strong resemblance with the spectrum photogenerated when the MLCT excited state reacts with TEA, Fig. 2. Since a concentration $[e^-_{solv}] \sim 2 \times 10^{-6}$ M of e^-_{solv} is generated in the pulse radiolysis experiments, only a small percentage (~1%) of the total number of –Re^I(CO)$_3$(bpy)$^+$ chromophores is reduced to –Re^I(CO)$_3$(bpy)$^{\bullet}$ by the solvated electrons. After the reaction of the e^-_{solv} with the polymer was completed, the absorption bands at λ_{max} = 450 and 490 nm remain nearly stable up to 1 ms (see Fig. 3). When solutions of ReP4VP were deaerated with streams of N_2O instead of N_2, all the radiolytically generated radicals were converted to C$^{\bullet}$H$_2$OH radicals in less than 1 μs. The radiolytic pulse caused only very small changes in the spectrum of the solution similar to those of Fig. 3. This experiment demonstrated that C$^{\bullet}$H$_2$OH radicals reduce the bpy ligand in ReP4VPy with a much lower efficiency than e^-_{solv} and that the absorbance changes in Fig. 3 are caused mainly by the reaction of e^-_{solv} with the Re^I pendants with only a minor (<10%) contribution from C$^{\bullet}$H$_2$OH radicals.

The extinction coefficient of the transients (ε_R) was calculated using the relationship

$$\varepsilon_R = \varepsilon_P + \frac{[\Delta A_R \times (G \times \varepsilon)(SCN)_2^{\bullet -}]}{[\Delta A(SCN)_2^{\bullet -} \times G_R]} \quad (5)$$

where ε_P is the extinction coefficient of the parent molecule, $\Delta A(SCN)_2^{\bullet -}$ is the absorbance of the thiocyanate radical at 472 nm and G_R is the radiation chemical yield of the radical. On this basis, $\varepsilon_{490\,nm} = 1.4 \times 10^3\ M^{-1}\ cm^{-1}$ was calculated for $-Re^I(CO)_3(bpy)^{\bullet}$.

We turn now to flash photolysis experiments. A growth of the $-Re^I(CO)_3(bpy)^{\bullet}$ spectrum within the first microsecond after the laser shot in flash photolysis experiments (inset to Fig. 2) can be explained by additional reduction of $-Re^I(CO)_3(bpy)^+$ groups by reducing TEA$^{\bullet}$ radicals generated by a reaction of TEA$^{\bullet +}$ with TEA [25] (Eqs. (6) and (7))

$$(CH_3CH_2)_3N^{\bullet +} + TEA \rightarrow (CH_3CH_2)_2N(^{\bullet}CHCH_3) + TEAH^+ \quad (6)$$

$$-Re^I(CO)_3(bpy)^+ + (CH_3CH_2)_2N(^{\bullet}CHCH_3) \rightarrow -Re^I(CO)_3(bpy)^{\bullet} + (CH_3CH_2)_2N{-}CH{=}CH_2 + H^+ \quad (7)$$

The demise of TEA$^{\bullet}$ radicals by disproportionation [26,27], Eq. (8), is in competition with the reduction process of Eq. (7)

$$2(CH_3CH_2)_2N(^{\bullet}CHCH_3) \rightarrow TEA + (CH_3CH_2)_2N{-}CH{=}CH_2 \quad (8)$$

With the aid of the extinction coefficient calculated above for $-Re^I(CO)_3(bpy)^{\bullet}$ and the ΔA_{max} of Fig. 2, it is estimated that the concentration of $-Re^I(CO)_3(bpy)^{\bullet}$ produced in flash photolysis experiments, $[-Re^I(CO)_3(bpy)^{\bullet}] \sim 1 \times 10^{-4}$ M, is between one and two orders of magnitude higher than the $[-Re^I(CO)_3(bpy)^{\bullet}]$ generated in pulse radiolysis experiments. This estimation is only a rough one for $[-Re^I(CO)_3(bpy)^{\bullet}]$ since it is assumed that the extinction coefficient of $-Re^I(CO)_3(bpy)^{\bullet}$ has the same value either in CH_3CN or MeOH. A disproportionation reaction of $-Re(CO)_3(bpy)^{\bullet}$ radicals [15–17,28], Eqs. (9) and (10), may occur sequentially

$$-Re^I(CO)_3(bpy)^{\bullet} + TEAH^+ \rightarrow -Re^I(CO)_3(bpyH)^{\bullet +} + TEA \quad (9)$$

$$2{-}Re^I(CO)_3(bpyH)^{\bullet +} \rightarrow -Re^I(CO)_3(bpyH_2)^+ + -Re^I(CO)_3(bpy)^+ \quad (10)$$

Eqs. (9) and (10) represent the protonation of $-Re^I(CO)_3(bpy)^{\bullet}$ by available $TEAH^+$ in the polymer and the slow diffusive motion of the polymeric strands that allows a bimolecular encounter of $-Re^I(CO)_3(bpyH)^{\bullet +}$ pendants, respectively. The whole process occurs in the millisecond–second time domain in pulse radiolysis experiments where the $-Re^I(CO)_3(bpy)^{\bullet}$ radical species are produced in low concentrations ($\sim 4 \times 10^{-6}$ M). Because the radicals will be separated from each other by large distances, diffusive motions of the polymer strands are required to bring them together. In flash photolysis experiments, however, the initial concentration of $-Re^I(CO)_3(bpy)^{\bullet}$ radical species generated by reductive quenching of the excited states by TEA is high ($\sim$15% of the total number of $Re^I(CO)_3(bpy)^+$ pendants) and diffusive motions are hardly required. In this condition, the disproportionation occurs much faster, i.e., in the microsecond time domain. As the decay of the $-Re^I(CO)_3(bpy)^{\bullet}$ radical species generated in flash photolysis experiments follows a first-order kinetics, Eq. (9) must be the rate determining step in the mechanism of Eqs. (9) and (10). This situation was previously encountered in the disproportionation of $-Re^I(CO)_3(phen)^{\bullet}$ radicals [28].

3.3. Estimation of the free energy (ΔG) for the forward electron transfer

For photoinduced electron transfer between an acceptor (A) and a donor (D) the energy balance of the forward electron transfer is given by [29]

$$\Delta G = N_A\{e[E_0(D^{\bullet +}/D) - E_0(A/A^{\bullet -})] + w(D^{\bullet +}A^{\bullet -}) - w(DA)\} - \Delta E_{0-0} \quad (11)$$

$$w(D^{\bullet +}A^{\bullet -}) = \frac{z(D^{\bullet +})z(A^{\bullet -})}{\varepsilon r} \quad (12)$$

$$w(DA) = \frac{z(D)z(A)}{\varepsilon r} \quad (13)$$

where $E^0(D^{\bullet +}/D)$ is the standard electrode potential of the donor cation radical resulting from the electron transfer, $E^0(A/A^{\bullet -})$ is the standard electrode potential of the acceptor (both relative to the same reference electrode), ΔE_{0-0} is the vibrational zero electronic energy of the excited state, e is the charge of an electron and N_A de Avogadro's number. In Eqs. (11)–(13) $w(D^{\bullet +}A^{\bullet -})$ and $w(DA)$ are the electrostatic work terms that account for the effect of Coulombic attraction in the products and reactants, respectively, ε is the static dielectric constant of the solvent and r is the distance of the charged species after electron transfer. In our system $w(D^{\bullet +}A^{\bullet -})$ and $w(DA)$ can be neglected since one of the reactants and/or products has no electric charge. Taking into account the standard electrode potential of the of the amines [30,31a] and of the complex $pyRe(CO)_3(bpy)^+$ [32] and the energy of the excited state ΔE_{0-0}, a calculation of the free energy (ΔG) for the forward electron transfer can be made using Eq. (11). The excited state energy was calculated in Ref. [14] from the luminescence spectrum of the complex $pyRe(CO)_3(bpy)^+$, giving a value of $\Delta E_{0-0} \sim 2.37$ eV [14]. This value compares well with the ΔE_{0-0} of $ClRe(CO)_3(bpy)$ (2.30 eV from [31c]) and that of ph-CO-HN-Bz-$pyRe(CO)_3(bpy)^+$ (2.38 eV from [31d]). The values of ΔG thus calculated are collected in Table 1.

3.4. Mechanism for the electron transfer

The following kinetic scheme may be considered for the forward electron transfer reaction [31a,31b]:

$$(A^+)^* + D \underset{k_{-d}}{\overset{k_d}{\rightleftarrows}} [(A^+)^*, D] \underset{k_{-e}}{\overset{k_e}{\rightleftarrows}} [(A^{\bullet}), D^{\bullet +}] \xrightarrow{k_p} A^{\bullet} + D^{\bullet +} \quad (14)$$

where k_d is the diffusion rate constant, k_{-d} is the dissociation rate constant, k_e and k_{-e} are the forward and backward electron transfer rate constants and k_p is the rate constant for pair separation. $(A^+)^*$ represents the acceptor (i.e., $pyRe(CO)_3(bpy)^+$ and/or pendants $-Re^I(CO)_3(bpy)^+$ in ReP4VPy) in its MLCT excited state and D the amine donor. The overall rate constant is written as [31b]:

$$k_q = \frac{k_d}{1 + (k_{-d}/k_e)(k_{-e}/k_p + 1)} \quad (15)$$

Introducing the Gibbs energy change for the electron transfer process [31b] (Eq. (16))

$$\frac{k_e}{k_{-e}} = \exp\left(-\frac{\Delta G}{RT}\right) \quad (16)$$

and $k_e = k_e^0 \exp(-\Delta G^*/RT)$, where $k_e^0 = \kappa \nu_N$, κ is the transmission coefficient of electron transfer which is 1 in the classical limit, and ν_N is the frequency factor, which varies from the order of 10^{12}–$10^{14}\ s^{-1}$ and can be approximated to be of the order of $10^{13}\ s^{-1}$ [31a]. ΔG^* is the activation free energy for the electron transfer step. Then, after substitution of k_e and Eq. (16) into Eq. (15) we can obtain Eq. (17)

$$k_q = \frac{k_d}{1 + (k_{-d}/\kappa\nu_N)\exp(\Delta G^*/RT) + (k_{-d}/k_p)\exp(\Delta G/RT)} \quad (17)$$

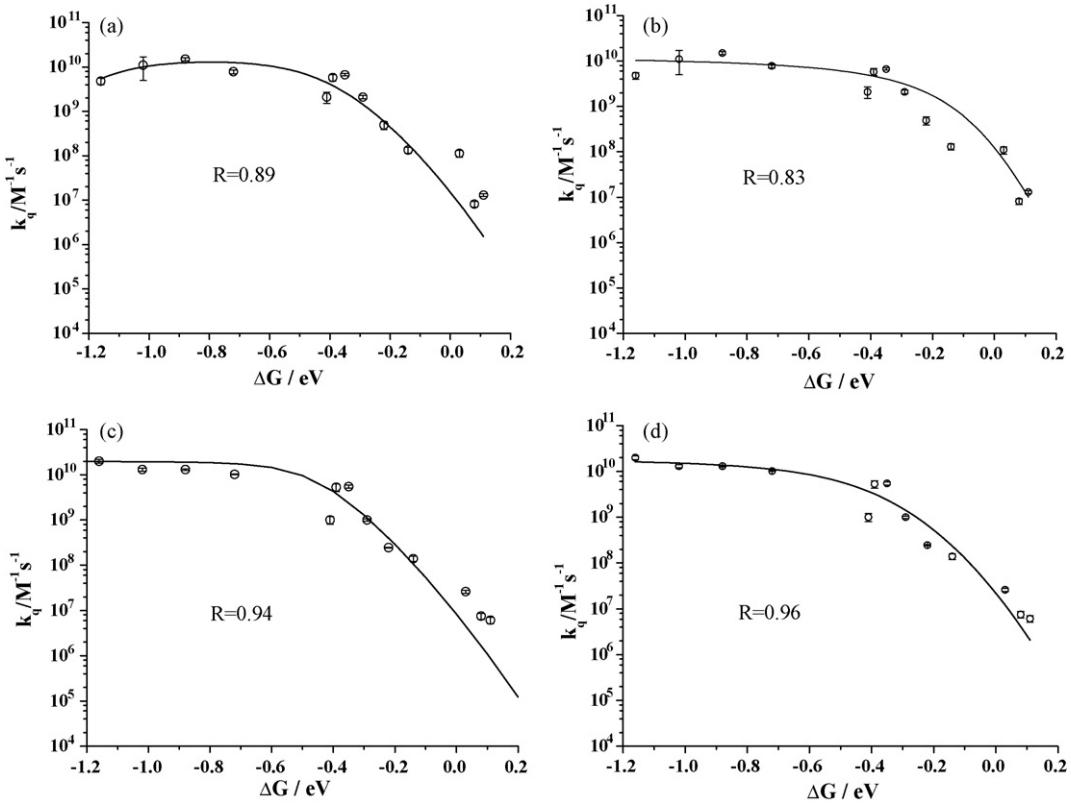

Fig. 4. Dependence of the quenching rate constant on ΔG for the MLCT luminescence quenching by amines. (a and b) $k_{q,2}$ vs. ΔG for ReP4VPy. The solid line in (a) shows the best fitting of the experimental data points to the Marcus expression of ΔG while the solid line in (b) shows the best fitting of the experimental data points to the Rehm–Weller expression of ΔG. (c and d) $k_{q,1}$ vs. ΔG for pyRe(CO)$_3$(bpy)$^+$. The solid line in (c) shows the best fitting of the experimental data points to the Marcus expression of ΔG while the solid line in (d) shows the best fitting of the experimental data points to the Rehm–Weller expression of ΔG. The values of κ and λ obtained by the curve fit analysis of (a–d) are collected in Table 2. See text for details.

Under the assumption that k_p is much larger than k_{-e}, which is supported by the observation of the –Re^{I}(CO)$_3$(bpy)$^{\bullet}$ radical species by flash photolysis experiments, the overall rate constant may be approximately written as:

$$k_q = \frac{k_d}{1 + (k_{-d}/\kappa\nu_N)\exp(\Delta G^*/RT)} \quad (18)$$

Several relationships between ΔG^* and ΔG have been proposed. In the classical parabolic Marcus [1,31a] equation ΔG^* becomes (Eq. (19))

$$\Delta G^* = \frac{(\lambda + \Delta G)^2}{4\lambda} \quad (19)$$

where $\lambda/4$ is the activation free energy when $\Delta G = 0$ (intrinsic barrier). Here λ, the total reorganization energy, is considered to be the sum of the inner sphere (λ_{in}) and solvent (λ_{out}) contributions:

$$\lambda = \lambda_{in} + \lambda_{out} \quad (20)$$

The solvent reorganization energy may be estimated by [31a]:

$$\lambda_{out} = e^2\left(\frac{1}{2r_D} + \frac{1}{2r_A} - \frac{1}{r_{DA}}\right)\left(\frac{1}{n^2} - \frac{1}{\varepsilon}\right) \quad (21)$$

where r_D and r_A are the radii of the donor and acceptor, r_{DA} is the distance between the donor and acceptor in the encounter complex, n is the refractive index of the solvent (1.34 for acetonitrile at 298 K [33]) and ε is the solvent dielectric constant (37.5 for acetonitrile at 298 K [33]). Using a mean value of r_D for all the amines [31a] and a value of r_A = 8 Å for pyRe(CO)$_3$(bpy)$^+$ from interatomic distances obtained from similar related Re^{I} compounds [17,34] a value of 0.7 eV may be estimated for λ_{out}.

The diffusion rate constant (k_d), calculated according to Smoluchowski [31a] for non-charged molecules, has a value of 2.0×10^{10} M^{-1} s^{-1} in acetonitrile. Following the Fuoss and Eigen equation [31a], K_d, i.e., the equilibrium constant of the encounter complex ($K_d = k_d/k_{-d}$) may be estimated as 5.4 M^{-1} and hence $k_{-d} = 3.7 \times 10^9$ s^{-1}.

However, in order to fit the experimental results for bimolecular charge separation reactions where the inverted effect predicted by the parabolic Marcus expression is not observed and asymptotic behavior is obtained for k_q at higher exoergonic reactions, an expression of ΔG^* that tends asymptotically toward zero for highly negative values of ΔG is necessary. The Rehm–Weller relationship [10], Eq. (22), meets this requirement.

$$\Delta G^* = \frac{\Delta G}{2} + \left[\left(\frac{\Delta G}{2}\right)^2 + \left(\frac{\lambda}{4}\right)^2\right]^{1/2} \quad (22)$$

3.5. Relationship between the rate constants and ΔG

In Fig. 4, $k_{q,1}$ and $k_{q,2}$ are plotted against ΔG. For pyRe(CO)$_3$(bpy)$^+$, the rate constants $k_{q,1}$ increase as the driving force becomes less positive, i.e., -0.6 eV < ΔG < 0.2 eV. However, when -1.2 eV < ΔG < -0.7 eV, $k_{q,1}$ reaches the diffusional value k_d and eventually an asymptotic plateau is obtained. Fig. 4 shows a similar behavior for ReP4VPy: $k_{q,2}$ increases as ΔG varies between 0.2 and -0.7 eV and it reaches the diffusional value at $\Delta G \sim -0.9$ eV. However, at more negative values, it shows "vestiges" of inverted region behavior. The $k_{q,2}$ value at $\Delta G = -1.15$ eV, which is 4.8×10^9 M^{-1} s^{-1}, is slightly lower than k_d, a situation often encountered in studies of bimolecular electron transfer reactions at high exothermicities. When one compares $k_{q,1}$ and

Table 2
Transmission electron coefficients (κ) and total reorganization energy (λ) for the quenching of the MLCT luminescence of pyRe(CO)$_3$(bpy)$^+$ and ReP4VPy by amines. *R* stands for the correlation coefficient for each fit of the experimental values of k_q for pyRe(CO)$_3$(bpy)$^+$/ReP4VPy with the Marcus and/or Rehm–Weller models of ΔG^*.

System	Model of ΔG^*	κ	λ/eV	*R*
pyRe(CO)$_3$(bpy)$^+$	Marcus	$(2 \pm 1) \times 10^{-2}$	1.2 ± 0.1	0.94
	Rehm–Weller	$(2 \pm 1) \times 10^{-2}$	1.1 ± 0.2	0.96
ReP4VPy	Marcus	$(7 \pm 1) \times 10^{-4}$	0.80 ± 0.03	0.89
	Rehm–Weller	$(9 \pm 5) \times 10^{-4}$	0.6 ± 0.2	0.83

$k_{q,2}$ values of Table 1, it is generally observed that $k_{q,2}$ is slightly higher than $k_{q,1}$ for values of $-0.6\,\text{eV} < \Delta G < 0.2\,\text{eV}$. The situation is reversed for $\Delta G < -0.7\,\text{eV}$ and $k_{q,1}$ becomes higher than $k_{q,2}$. In fitting the experimental k_q values with either the Marcus and/or Rehm–Weller model for ΔG^*, it was observed that $k_{q,1}$ values were better fitted by the Rehm–Weller model (Fig. 4d) while $k_{q,2}$ values were better represented by the Marcus model (Fig. 4a) for ΔG^*, as it is suggested by the correlation coefficients of Table 2 and Fig. 4. Fig. 4a–d shows the best fitting of the experimental data points to the Marcus and Rehm–Weller expression of ΔG using Eqs. (18) and (19) and Eqs. (18) and (22), respectively. The best fit was obtained using a $k_d = 2 \times 10^{10}\,\text{M}^{-1}\,\text{s}^{-1}$ and the values of κ and λ are collected in Table 2.

In spite of the fact that the Marcus model seems to describe better the k_q relationship with ΔG for ReP4VPy while the Rehm–Weller model seems better for pyRe(CO)$_3$(bpy)$^+$ both models are coincident in two aspects: (i) the total reorganization energy (λ) is higher by about 0.3–0.5 eV for pyRe(CO)$_3$(bpy)$^+$ than for ReP4VPy; (ii) the quenching reaction of MLCT by amines is a non-adiabatic reaction ($\kappa \sim 1 \times 10^{-3}$–$1 \times 10^{-2}$). At this point it is important to recall that transmission electron microscopy and dynamic light scattering studies on acetonitrile solutions of ReP4VPy demonstrated that the Re^I-polymer molecules aggregate to form spherical nanoaggregates of radius $R \sim 156$ nm [14]. It is well known that the motion of the solvent molecules in the restricted media, i.e., in micelles and/or nanodomains, is retarded by several orders of magnitude compared to that in homogeneous solvents. Thus the solvent reorganization may not contribute completely within the time scale of the electron transfer reaction between the ReP4VPy's MLCT and amines. Therefore, higher values of λ are expected for pyRe(CO)$_3$(bpy)$^+$ than for ReP4VPy in accordance with the values shown in Table 2. According to Marcus expression for ΔG^*, in the normal region, where $\Delta G < \lambda$, the limiting value of ΔG^* from Eq. (19) tends to $\Delta G^* \sim 1/2(\Delta G) + 1/4(\lambda)$. Since λ is higher for pyRe(CO)$_3$(bpy)$^+$ than for ReP4VPy then $k_{q,2} \geq k_{q,1}$. However, the fact that the $k_{q,2} \geq k_{q,1}$ for most of the amines studied may be reflecting also a contribution from the polymer backbone to a decrease of the inner sphere reorganization energy (λ_{in}) of the electron transfer process via vibrational modes of the uncomplexed pyridines in the polymer backbone. Nevertheless, a higher value of k_q in ReP4VPy than in pyRe(CO)$_3$(bpy)$^+$ may also be explained due to the fact that the diffusion of the amine molecules to form the encounter complex with the –Re(CO)$_3$(bpy)$^+$ chromophore is favoured –compared to pyRe(CO)$_3$(bpy)$^+$ – due to the fact that the amine might have a certain tendency to be close to the polymer by hydrogen bonding interactions with the free pyridine groups and may thus more often encounter –Re(CO)$_3$(bpy)$^+$ than in the case of pyRe(CO)$_3$bpy$^+$. The three effects may be contributing simultaneously to the fact that $k_{q,2} \geq k_{q,1}$ in the normal region. At higher exothermicities, i.e., in the so-called inverted region ($-\Delta G > \lambda$), the absence of a solvent reorganization in the quenching of ReP4VPy's MLCT luminescence by amines may explain a slight tendency of $k_{q,2}$ to decrease while $k_{q,1}$ reaches a plateau at the diffusional k_d value.

According to quantum mechanical expressions of electron transfer theory the splitting that occurs at the intersection of the potential-energy surfaces of reactants and products is crucial for electron transfer. This splitting is equal to $2H_{rp}$, where H_{rp} is the electronic coupling matrix element $\langle \Psi_r | H_{el} | \Psi_p \rangle$, Ψ_r and Ψ_p being the electronic wave functions of the equilibrium reactant and product states, respectively, and H_{el} is the electronic Hamiltonian [35]. The electronic transmission coefficient (or electronic factor) is proportional to H_{rp}^2 and attains a maximum value of $\kappa = 1$ at large enough values of H_{rp}. The total electronic wave function must include the spatial and spin wave functions and the electronic matrix element may be factorised in a spatial and a spin factor. The spin factor is different from zero for states of the same multiplicity. Therefore values of $\kappa \ll 1$ are expected if the spin multiplicities of Ψ_r and Ψ_p are different. In the present case, the MLCT of a –Re(CO)$_3$bpy$^+$ chromophore, which has triplet character [36,37], is quenched by the singlet ground state of an amine and the products are doublets in spin multiplicity (Eqs. (23) and (24))

$$^3[\text{–Re(CO)}_3\text{bpy}^+]^* + \text{NR}_3 \underset{k_{-d}}{\overset{k_d}{\rightleftarrows}} {}^3[\text{pyRe(CO)}_3\text{bpy}^+, \text{NR}_3] \underset{k_{-e}}{\overset{k_e}{\rightleftarrows}} {}^3[{}^2(\text{–Re(CO)}_3\text{bpy}^\bullet), {}^2\text{NR}_3{}^{\bullet+}] \quad (23)$$

$$^3[{}^2(-\textit{Re}\text{(CO)}_3\text{bpy}^\bullet), {}^2\text{NR}_3{}^{\bullet+}] \xrightarrow{k_p} {}^2[\text{–Re(CO)}_3\text{bpy}^\bullet] + {}^2\text{NR}_3{}^{\bullet+} \quad (24)$$

Therefore the coupling matrix element $\langle \Psi_r | H_{el} | \Psi_p \rangle$ may include coupling between states of differing multiplicity and H_{rp}^2 may be small and then $\kappa \ll 1$. However, the electron transfer process may become enhanced through spin–orbit coupling [35] which mixes the wave functions for intermediate spin states with the wave functions for the initial (or final) states (Eqs. (25) and (26))

$$\Psi = \Psi_r + c\Psi_p \quad (25)$$

$$c = \frac{\langle \Psi_r | H_{so} | \Psi_p \rangle}{E_r - E_p} \quad (26)$$

where c is the mixing coefficient, H_{so} is the spin–orbit interaction operator, and E_p and E_r are the energies of the intermediate and initial (or final) spin states. Since rhenium is a heavy metal, enhanced spin–orbit coupling occurs, which leads to values of $\kappa \sim 1 \times 10^{-3}$–$1 \times 10^{-2}$ that may be observed experimentally in the luminescence quenching of ^{3}[MLCT] by amines.

4. Conclusions

The MLCT luminescence quenching of pyRe(CO)$_3$bpy$^+$ and ReP4VPy by amines proceeds via an electron transfer reaction which produces amine cation radicals and pyRe^I(CO)$_3$(bpy)$^\bullet$/–Re^I(CO)$_3$(bpy)$^\bullet$, respectively. The observed rate constants, i.e., $k_{q,1}$ and $k_{q,2}$ may be described in terms of the ΔG of the electron transfer reaction either by the Marcus or the Rehm–Weller models for ΔG^*. However, Marcus model seems to describe better the behavior of the system ReP4VPy/amines while the Rehm–Weller model seems better for the system pyRe(CO)$_3$bpy$^+$/amines. The formation of nanoaggregates of ReP4VPy polymer strands, thus reducing the total reorganization energy, explains satisfactorily the differences encountered

between $k_{q,1}$ and $k_{q,2}$, i.e., higher values of $k_{q,2}$ than $k_{q,1}$ in the normal region and a slight tendency of ReP4VPy to follow a parabolic behavior at high exothermicities. The observed dispersion of the data could be related, at least in part, to differences in the internal reorganization energy for each amine. Moreover, some contribution of the uncertainty of the irreversible oxidation potentials of the aliphatic amines cannot be disregarded.

Acknowledgements

Work supported in part by ANPCyT Grant No. PICT 26195, CONICET-PIP 6301/05, Universidad Nacional de La Plata, and CICPBA. Flash photolysis and pulse radiolysis experiments were done at the Notre Dame Radiation Laboratory, Indiana, USA. E.W. thanks Dr. Guillermo Ferraudi for hosting his visit to NDRL. L.L.B.B. acknowledges support from CONICET. E.W. is a member of CONICET and M.R.F. is a member of CICPBA.

References

[1] R.A. Marcus, Discuss. Faraday Soc. 29 (1960) 21.
[2] R.A. Marcus, J. Photochem. Photobiol. A: Chem. 82 (1994) 1–3.
[3] (a) J.V. Beitz, J.R. Miller, J. Chem. Phys. 71 (1979) 4579–4595;
(b) J.R. Miller, J.V. Beitz, R.K. Huddleson, J. Am. Chem. Soc. 106 (1984) 5057–5068;
(c) G.L. Closs, L.T. Calcaterra, N.J. Green, K.W. Penfield, J.R. Miller, J. Phys. Chem. 90 (1986) 3673–3683;
(d) G.L. Closs, J.R. Miller, Science 240 (1988) 440–447.
[4] (a) I.R. Gould, D. Ege, S.L. Mattes, S. Farid, J. Am. Chem. Soc. 109 (1987) 3794–3796;
(b) I.R. Gould, J.E. Moser, B. Armitage, S. Farid, J.L. Goodman, M.S. Herman, J. Am. Chem. Soc. 111 (1989) 1917–1919;
(c) I.R. Gould, R. Moody, S. Farid, J. Am. Chem. Soc. 110 (1988) 7242–7244.
[5] (a) M.P. Irvine, R.J. Harrison, G.S. Beddard, P. Leighton, J.K.M. Sanders, Chem. Phys. 104 (1986) 315–324;
(b) G. Tapolsky, R. Duesing, T.J. Meyer, J. Phys. Chem. 93 (1989) 3885–3887;
(c) P.Y. Chen, R. Duesing, G. Tapolsky, T.J. Meyer, J. Am. Chem. Soc. 111 (1989) 8305–8306;
(d) P.Y. Chen, R. Duesing, D.K. Graft, T.J. Meyer, J. Phys. Chem. 95 (1991) 5850–5858.
[6] (a) N. Mataga, T. Asahi, Y. Kanda, T. Okada, T. Kakitani, Chem. Phys. 127 (1988) 249–261;
(b) T. Ohno, A. Yoshimura, N. Mataga, J. Phys. Chem. 90 (1986) 3295–3297;
(c) T. Ohno, A. Yoshimura, N. Mataga, J. Phys. Chem. 94 (1990) 4871–4876.
[7] (a) D.Y. Yang, R.I. Cukier, J. Chem. Phys. 91 (1989) 281–292;
(b) M.R. Gunner, P.L. Dutton, J. Am. Soc. 111 (1989) 3400–3412;
(c) T.J. Meade, H.B. Gray, J.R. Winkler, J. Am. Chem. Soc. 111 (1989) 4353–4356;
(d) L.S. Fox, M. Kozik, J.R. Winkler, H.B. Gray, Science 247 (1990) 1069–1071.
[8] (a) C. Creutz, N. Sutin, J. Am. Chem. Soc 99 (1977) 241–243;
(b) T.B. Truong, J. Phys. Chem. 88 (1984) 3906–3913;
(c) P.P. Levin, P.F. Pluzhnikov, V.A. Kuzmin, Chem. Phys. Lett. 147 (1988) 283–287.
[9] M. Kumbhakar, S. Nath, T. Mukherjee, H. Pal, J. Chem. Phys. 120 (2004) 2824–2834.
[10] D. Rehm, A. Weller, Isr. J. Chem. 8 (1970) 259–271.
[11] (a) E. Wolcan, M.R. Féliz, Photochem. Photobiol. Sci. 2 (2003) 412–417;
(b) Abbreviations used in this work: bpy = 2,-2′-bipyridine, py = pyridine, ph = phenyl, vpy = vinylpyridine, Bz-py = 4-benzyl-pyridine, SE = standard error.
[12] S. Hou, W.K. Chan, Macromol. Rapid Commun. 20 (1999) 440–443.
[13] S. Hou, K.Y.K. Man, W.K. Chan, Langmuir 19 (2003) 2485–2490.
[14] E. Wolcan, J.L. Alessandrini, M.R. Féliz, J. Phys. Chem. B 109 (2005) 22890–22898.
[15] M.R. Féliz, G. Ferraudi, J. Phys. Chem. 96 (1992) 3059–3062.
[16] M.R. Féliz, G. Ferraudi, H. Altmiller, J. Phys. Chem. 96 (1992) 257–264.
[17] J. Guerrero, O.E. Piro, E. Wolcan, M.R. Féliz, G. Ferraudi, S.A. Moya, Organometallics 20 (2001) 2842–2853.
[18] G.F. De Sá, L.H.A. Nunes, Z.-M. Wang, G.R. Choppin, J. Alloys Compd. 196 (1993) 17–23.
[19] G.L. Hug, Y. Wang, C. Schöneich, P.-Y. Jiang, R.W. Fessenden, Radiat. Phys. Chem. 54 (1999) 559–566.
[20] G.V. Buxton, C.L. Greenstock, W.P. Helman, A.B. Ross, J. Phys. Chem. Ref. Data 17 (1988) 513–886.
[21] M.R. Féliz, G. Ferraudi, Inorg. Chem. 37 (1998) 2806–2810.
[22] N. Getoff, A. Ritter, F. Schwörer, P. Bayer, Radiat. Phys. Chem. 41 (1993) 797–801.
[23] L.M. Dorfman, in: R.F. Gould (Ed.), The Solvated Electron in Organic Liquids, Advances in Chemistry Series 50, American Chemical Society, Washington, DC, 1965, pp. 36–44.
[24] M. Simic, P. Neta, E. Hayon, J. Phys. Chem. 73 (1969) 3794–3800.
[25] C. Kutal, M.A. Weber, G. Ferraudi, D. Geiger, Organometallics 4 (1985) 2161–2166.
[26] M. Goez, I. Sartorius, J. Am. Chem. Soc. 115 (1993) 11123–11133.
[27] M. Goez, I. Sartorius, J. Phys. Chem. A 107 (2003) 8539–8546.
[28] E. Wolcan, G. Ferraudi, J. Phys. Chem. A 104 (2000) 9281–9286.
[29] S.E. Braslavsky, Pure Appl. Chem. 79 (2007) 293–465.
[30] (a) M.V. Encinas, S.G. Bertolotti, C.M. Previtali, Helv. Chim. Acta 85 (2002) 1427–1438;
(b) V. Solis, T. Iwasita, M.C. Giordano, J. Electroanal. Chem. 105 (1979) 169–179;
(c) J.W. Arbogast, C.S. Foote, M. Kao, J. Am. Chem. Soc. 114 (1992) 2277–2279.
[31] (a) G. Ruiz, F. Rodriguez-Nieto, E. Wolcan, M.R. Féliz, J. Photochem. Photobiol. A 107 (1997) 47–54;
(b) G. Porcal, S.G. Bertolotti, C.M. Previtali, M.V. Encinas, Phys. Chem. Chem. Phys. 5 (2003) 4123–4128;
(c) K. Kalyanasundaram, in: K. Kalyanasundaram, M. Grätzel (Eds.), Photosensitization and Photocatalysis Using Inorganic and Organometallic Compounds, Kluwer Academic Publishers, 1993, p. 126;
(d) K.S. Schanze, D. Brent MacQueen, T.A. Perkins, L.A. Cabana, Coord. Chem. Rev. 122 (1993) 63–89.
[32] L.A. Sacksteder, A.P. Zipp, E.A. Brown, J. Streich, J.N. Demas, B.A. DeGraff, Inorg. Chem. 29 (1990) 4335–4340.
[33] J.A. Riddick, W.B. Bunger, Organic Solvents, Techniques of Chemistry, 4th ed., Wiley Interscience, New York, 1986.
[34] N. Murakami-Iha, G. Ferraudi, J. Chem. Soc., Dalton Trans. (1994) 2565–2571.
[35] N. Sutin, Acc. Chem. Res. 15 (1982) 275–282.
[36] E. Wolcan, M.R. Féliz, J.L. Alessandrini, G. Ferraudi, Inorg. Chem. 45 (2006) 6666–6677.
[37] L.L.B. Bracco, M.P. Juliarena, G.T. Ruiz, M.R. Féliz, G.J. Ferraudi, E. Wolcan, J. Phys. Chem. B 112 (2008) 11506–11516.